UNIVERSITY OF THE
WITWATERSRAND,
JOHANNESBURG

SCHOOL OF MECHANICAL,
INDUSTRIAL & AERONAUTICAL
ENGINEERING

MECHATRONICS II: MECN4029A

MECHATRONIC SYSTEMS DESIGN: ANALYSIS AND CONTROL
PROJECT B: SOLAR TRACKER

GROUP 11

Netshisumbewa Mpho	**1825498**
Petersen Waylin	**1884672**
Mphaga Gumani	**2129552**
Nkabinde Sandiswa	**2324218**

UNIVERSITY OF THE WITWATERSRAND, JOHANNESBURG

SCHOOL OF MECHANICAL, INDUSTRIAL & AERONAUTICAL ENGINEERING

Disclosure – Use of Artificial-Intelligence (AI) Generated Content

2024 V2

Students must acknowledge all use of AI.

Select all applicable statements and complete the sections fully. Delete all statements that are not applicable.

1. Disclosure: No AI use

☒ I acknowledge that no AI tools/technologies (Grammarly, ChatGPT, Bard, Quillbot, OpenAI etc) were used in the completion of this assessment.

☒ ***I declare that the disclosure is complete and truthful.***

Student number:
1825498
1884672
2129552
2324218
Course code: MECN4020A
Date: 20/05/2024

Executive Summary

This report details the work done to design a sun tracking solar system for the Apex student accommodation in Braamfontein. The solar system was model in 2 parts mainly the electromechanical part from the motor and the mechanical part from the panel itself. The system was defined by one global equation, and it was then linearized to assist with the system analysis. The stability of the system was analysed using various methods such as the routh tables, bode plot, and pole zero plot. A controller was implemented after the results showed that it was indeed needed. Sun position data was sourced and then integrated into the model of which the controller followed the sun's position. This was done for the data throughout the day. Recommendations were such that to accommodate the building's needs, multiple systems would need to be installed to increase the power output.

TABLE OF CONTENTS

List of figures

List of tables

1 Introduction

1.1 Project background

The project was undertaken to develop a single axis solar tracker which will enable sun tracking throughout the day, tracking of the sun can be done with either the aid of primary axis which can either be elevation or azimuth. The design of the control system should ensure that the solar panels are positioned to receive maximum sunlight throughout the day [1]. Figure 1 shows the solar installed on the roof to maximize the exposure to sunlight.

Figure 1: Solar Panels angled to maximize exposure to sun [2].

Solar tracking devices are currently in demand due to power crisis globally, research is being undertaken pertaining solar tracking and suitable configurations that will enable harnessing of sun's energy to the maximum. Use of solar tracker which rotates itself towards the direction of sunlight for maximum power capturing maximizes the use of solar panel [3]. Control systems is often integrated in the solar tracking systems as the systems are not manually controlled. This paper focuses on development of ideal configuration of the solar panel based on specified geographical location and implementation of efficient single axis solar tracker.

1.2 Scenario

With the loadshedding crisis at its peak in South Africa, many businesses have been taking a toll due to this. The Apex student's accommodation in Braamfontein is no exception. With a population of about 900 students, the management has seen it fit to implement a backup system to enable their students to continue with their normal activities even during power outages. It has been proposed that solar panels will be used and to maximize the system's efficiency, a system that tracks the sun's position has been listed as one of the requirements. This means that there is a task to develop a solar system which will be able to track the sun's position and self-adjust to maximize the harnessing of energy from the sun.

The panel configuration and support should be designed as such there would be adequate movement or rotation of the panel to allow maximum harnessing of the sun's energy. The configuration should also be able to be accommodative of components that will aid in efficient functioning of the system. Modelling of the system is based on principles covered in MECN 4029A (Mechatronics II) course. The final design of the control system should be able to provide positioning of the panel that will enable maximum harnessing of sunlight throughout the day.

2 Solar tracker specifications

The specifications for the solar panel model determine the performance, behaviour and limitations of the model under different conditions. Incorrectly specified parameters will yield unwanted performance and behaviour of the models with unrealistic limitations. The project tasks involve analysis of performance in both time and frequency domain, (time and frequency domain specification will be included for their respective analysis) and the analysis will be compared with simulation results to evaluate if the control is necessary or not, and if it is, how much of it is needed.

2.1 Performance Specifications

- The solar panel should be able to stabilize in set angle during sun tracking without readjusting due to external forces.
- The panel should adjust in short period of time for maximum harnessing of sunlight.
- The panel moment of inertia should allow the system to be correctly positioned without opposing the direction of orientation and putting strain in joints.

2.2 Time domain specifications

This performance criteria are concerned with behaviour of the system over time. The following characteristics are considered:

- Maximum overshoot
- Peak time
- Settling time, and
- Rise time

The maximum overshoot measures the maximum deviation of the output (y) by which the response of the system exceeds its steady-state value during transient response to rapid change in input [2]. This parameter is dependent on damping ratio of the system, and it can be minimized by choosing adequate damping ratio.

$$Maximum\ overshoot\ = \frac{y(t_p)-y(\infty)}{y(\infty)} *100\% \qquad (1)$$

Peak time is the time taken for system's output to rise from 0 to the first maximum value during its response [2]. This parameter is directly proportional to maximum overshoot and equation 2 is used to define it.

$$t_p = \frac{\pi}{\omega_n\sqrt{1-\zeta^2}} \qquad (2)$$

Settling time is the time taken for system's output to reach and remain within a specified small percentage of the final steady-state value [2].

$$t_s = \frac{4}{\zeta\omega_n} \qquad (3)$$

Rise time is the time taken for the system output to rise from a specified low percentage to a high specified percentage of its final value. This time is usually required to be small and is defined by equation 4.

$$t_r = \frac{\pi}{2\omega_d} \quad (4)$$

Steady state error is the difference between desired value and actual output value of a system once it has reached steady state.

The desired specifications are presented in Table 2.

Table 1 Time-domain performance specifications

Maximum overshoot (%)	≤ 15% steady state
Peak time (s)	< 0.5
Settling time (s)	< 2
Rise time (s)	< 0.5
Steady state error	5%

2.3 Frequency domain specifications

These performance criteria are concerned with characteristics of system frequency response. The following characteristics are considered and specifications for the model are summarised in Table 3.

- Bandwidth
- Amplitude ratio
- Peak amplitude ratio
- Resonant frequency

The desired specifications are presented in Table 3

Table 2 Frequency-domain performance specifications

Bandwidth (rad/s)	5 - 10
Amplitude Ratio	$0 \leq M_p \leq 2$
Peak amplitude ratio	$1 \leq x \leq 1.5$
Resonant frequency (rad/s)	23.56

3 Solar tracker modelling

3.1 Physical modelling of the panel

The solar panel being designed consists of both mechanical and electrical components; it can then be classified as an electromechanical system. The main components of the panel include the solar panel, the pole for support, one electric motor, spur gear arrangement and power supply components as well as the control unit for the system. The other components including hinges and supports can be considered as secondary components.

The design of the solar panel was chosen to lower the mass moment of inertia and lower its effect when the panel angle increases, hence connection is centred. The design and positioning of the hinges also allows ease of rotation of the solar panel with no obstructions. The height of the pole was slightly lowered to limit the effect of wind on the system based on the geographical location of the system and as it was assumed that the panels will be installed on the rooftop of a high-rise building. Table 3 highlights the physical specifications of the components which will be used for the mathematical modelling of the entire system.

Table 3 Physical Model Specification [4] [5] [6]

Parameter	**Corresponding value**
Motor torque constant (K_t)	0,077677 $N.m/A$
Motor mass moment of inertia (J)	0.6667 $kg.m^2$
Motor viscous damping constant (C_m)	0.000214 Ns/m
Circuit resistance (R_a)	0.46 $Ohms$
Circuit Inductance (L_a)	0.98 mH
Motor voltage constant (K_e)	0,005790 N. m/A
Rated operating voltage (V)	24 (V)
Panel damping constant (C_p)	0.006 Ns/m
Gear Ratio	1:60
Mass panel (M_p)	12.2 kg
Moment of inertia of panel (J_p)	2.2887 m^4
Dimensions (mm)	2278 × 1133 × 35 mm

3.2 Mathematical modelling of the system

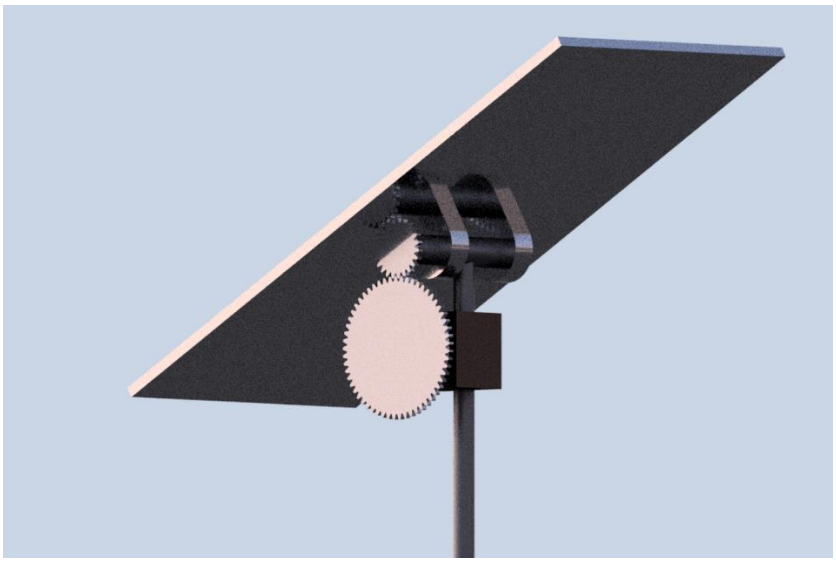

Figure 2: Model of the Panel

For the mathematical modelling, the system is considered to its entirety with both mechanical and electrical components being analysed to determine the overall relationship between components as they work together to as an electromechanical system.

Several assumptions were made to narrow the system down to its simplest form, the following assumptions were made:

- The panel will reach no more than 45 degrees tilt on both sides for maximum harnessing of sunlight throughout the day.
- The effect of the wind is very small due to the height of the pole where the panel is mounted, and small angle increase for the panel.
- Viscous friction was assumed to be present on the bearings attached to the joints facilitating smoother rotation of the panel.
- Energy losses from the motor were considered negligible.
- The elasticity of the structure was considered to be very small and thus can be neglected.
- No spring effects were considered in the system.
- Gear losses between the gears were neglected.
- The environment was assumed to be independent of system motion [7]
- The motor was assumed to directly impose the torque to the load.
- Mass moment of inertia and viscous friction on the joints were assumed to be the main forces acting on the system.

3.2.1 Mechanical System Equation of Motion

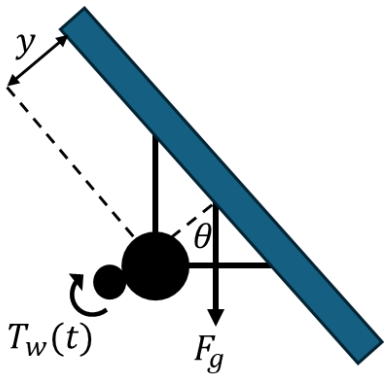

Figure 3: Mechanical System Schematic

$$\frac{d^2\theta}{dt^2} = \frac{1}{J}(T_p + yF_g \sin\theta - c * \frac{d\theta}{dt}) \quad (1)$$

$$J_p\ \ddot{\theta}(t) = T_\omega(t) + yF_g\theta(t) - c\dot{\theta}(t) \quad (2)$$

Equation 1 into 2:

$$T_\omega(t) + yF_g\theta_r(t) - c_p\dot{\theta}_r(t) = k_t i_a - c_m\dot{\theta}_r(t)$$

$$J_p\ \ddot{\theta}(t) = G_r\big[\, k_t i_a - c_m\dot{\theta}_r(t)\big] + yF_g\theta_p - c_m\dot{\theta}_r(t)$$

3.2.2 Electrical Systems Equations of Motion

For the Electrical components of the system, a suitable motor should be used and the resulting evaluated equation of the electrical side of the system can be related with the mechanical side of the system to yield final equation relating both the electrical and mechanical side of the system. Field-Controlled DC Motor and Armature-Controlled DC Motor were studied in Mechatronics II course and thus the selection will be based on the two. The Armature-Controlled DC Motor was chosen as a suitable motor to use due to its ability to keep the torque constant by simply keeping the armature current constant as mentioned by [8].

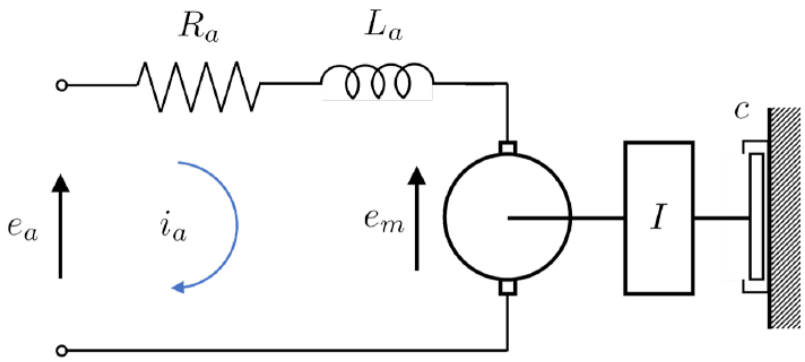

Figure 4: Armature-Controlled DC Motor [3]

Considering the load inertia and its angular displacement, the motor torque can be represented by:

$$T(t) = J\frac{d^2\theta(t)}{dt^2} + c\frac{d\theta(t)}{dt} \tag{3.1}$$

I: *Inertia of the motor*

c: *Damping constant*

Applying Kirchhoff's Law around the loop, the following equation is obtained:

$$e_a = R_a i_a + L_a\frac{di_a}{dt} + e_m \tag{3.2}$$

$$e_m = k_e\dot{\theta} \tag{3.3}$$

Torque developed by the motor is given by:

$$T(t) = K_t i_a \tag{3.4}$$

Final equations of the Armature-Controlled DC Motor:

$$K_t i_a = J\frac{d^2\theta(t)}{dt^2} + c\frac{d\theta(t)}{dt}$$

$$e_a = R_a i_a + L_a\frac{di_a}{dt} + k_e\frac{d\theta(t)}{dt}$$

Laplace was applied on the above equations assuming zero initial conditions to yield the following:

$$K_t I_a(s) = Js^2\theta(s) + cs\theta(s)$$

$$K_t I_a(s) = \theta(s)[Js^2 + cs]$$

$$I_a(s) = \frac{\theta(s)[Js^2+cs]}{K_t} \tag{3.5}$$

$$E_a(s) = R_a I_a(s) + L_a s I_a(s) + k_e s\theta(s)$$

$$E_a(s) = I_a(s)[R_a + L_a s] + k_e s\theta(s) \tag{3.6}$$

Equation 3.5 can be substituted into equation 3.6 to eliminate $I_a(s)$, therefore:

$$E_a(s) = \frac{\theta(s)[J + cs]}{K_t}[R_a + L_a s] + k_e s\theta(s)$$

$$E_a(s) = \theta(s)[\frac{J + cs}{K_t}(R_a + L_a s) + k_e s]$$

$$E_a(s) = \theta(s)[\frac{(J + cs)(R_a + L_a s)}{K_t} + k_e s]$$

Transfer function of the motor:

$$G(s) = \frac{\theta(s)}{E_a(s)} = \frac{K_t}{[(Js^2 + cs)(R_a + L_a s) + K_t k_e s]} \quad (3.7)$$

3.5. Linearization of the model

Moving forward from determining both mechanical and electrical system equations, the two were related via the gear transfer in order to have one equation defining the whole system. The combining of these equations was done 2 ways. Firstly, the model was defined in Simulink using the nonlinear equations from the previous section. The second part was done with the linearized equations making the overall equation linear. The two methods are outlined below.

3.5.1 Non-linear mathematical model:

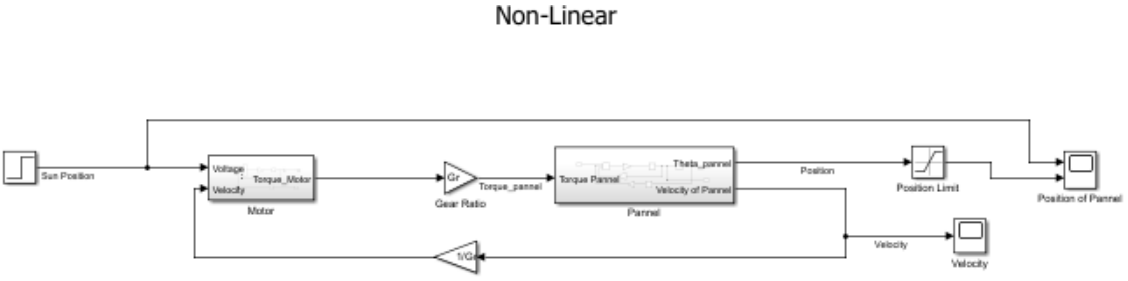

Figure 5: Simulink Non-Linear model

3.5.2 Linear mathematical model:

The relating of the motor and panel equations using the motor's torque yielded the following equation.

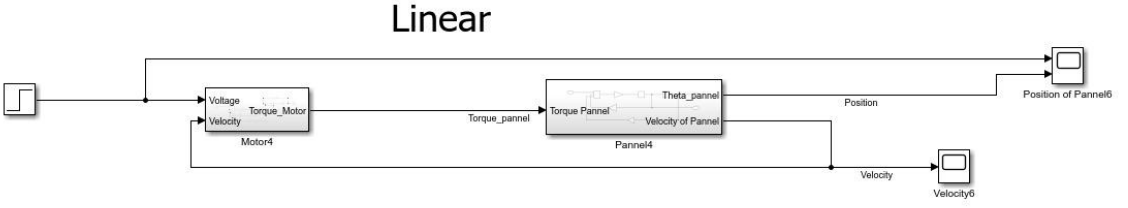

Figure 6: Linear Model Block diagram

$$J_p\,\ddot{\theta}(t) = G_r\big[\,k_t i_a - c_m\dot{\theta}_r(t)\big] + yF_g\theta_p - c_m\dot{\theta}_r(t)$$

Linearizing:

$$F\big(i_a, \dot{\theta}_m, \theta_r, \dot{\theta}_p, \ddot{\theta}_m\big) = J_p\ddot{\theta}_p - G_r k_t i_a + G_r c_m\dot{\theta}_m - yF_g\theta_p + c_m\dot{\theta}_p$$

Initial conditions: $\ddot{\theta}_p = 0$, $\dot{\theta}_m = 0$, $\dot{\theta}_p = 0$;

$F(0)$:

$$\frac{\partial F}{\partial i_a} = -(G_r k_t)\delta i_a$$

$$\frac{\partial F}{\partial \dot{\theta}_m} = G_r c_m \Delta\dot{\theta}_m$$

$$\frac{\partial F}{\partial \theta_p} = -yF_g\Delta\theta_p$$

$$\frac{\partial F}{\partial \dot{\theta}_p} = c_p\Delta\theta_p$$

$$\frac{\partial F}{\partial \dot{\theta}_p} = J_p\Delta\ddot{\theta}_p$$

$$0 = J_p\Delta\ddot{\theta}_p + c_p\Delta\theta_p - yF_g\Delta\theta_p + \frac{1}{G_r c_m\dot{\theta}_m} - \frac{1}{G_r k_t\Delta i_a}$$

$$\left[J_p s^2 + c_p s - yF_g + {G_r}^2 c_m s + \frac{k_e {G_r}^2}{L_a s + R_a}\right]\theta_p = \left[\frac{G_r k_e}{L_a s + R_a}\right]V(s)$$

$$G(s) = \frac{\theta(s)}{V(s)} = \frac{\frac{G_r k_t}{L_s + R}}{[(J_p)s^2 + (C_p + G_r^2 C_m)s + (\frac{k_e G_r^2}{L_s + R} - yF_g)]}$$

4 System Response analysis of uncontrolled model

The system response of the uncontrolled system will be analysed in both time and frequency domains with these performances later evaluated. To do the responses properly, the constant parameters that appear in the overall equations needed to be defined. These were sourced according to the components that were proposed in the earlier section. The summary of all these is listed in table 3 under section 3.1. Using those constants and parameters, the Simulink model was finally fully defined with constants and the final linear transfer function was also obtained with its values. These two were then used to produce the system's response under various inputs and the results are presented in this section.

4.1 Non-linear analysis

Realistic systems are naturally non-linear hence they require non-linear analytical models to be analysed. The analysis of the plant was performed using Simulink and the approach that was employed for modelling is block diagram technique shown in Figure 12 which used the equations of motions derived in section 3.

4.1.1 Time domain analysis

It is essential to analyse the equations that describe a system to gain a thorough understanding of its behaviour and performance. The analytical equations developed for both non-linear and linear model were simulated for uncontrolled plant. This analysis was performed in both the time domain, which examines the system's behaviour over time, and the frequency domain, which analyses the system's behaviour at various frequencies. By examining the system from both perspectives, a deeper insight can be gained into its dynamics and potential issues can be identified. This would help in designing more effective control strategies hence improved performance and enhanced stability.

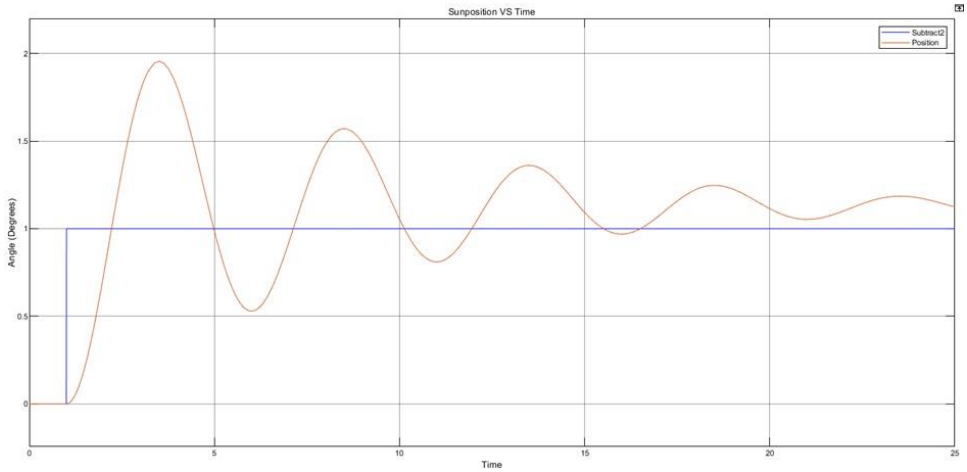

Figure 7: Non-linear response with time

From the Figure it could be seen that that when there is an abrupt change in input the system stability is disturbed and responds in damped oscillation. The system response shoots up from zero degrees to 1.8 degrees in 3 seconds. After 3 seconds then it comes down until it is close to 0.5 degrees, then it oscillates again in a damped manner until it converges to one output which is around 1.2 degrees after 20 seconds and it then reaches equilibrium. Then the system remains at this angle until there is another abrupt change in the input again.

- System response visualisation

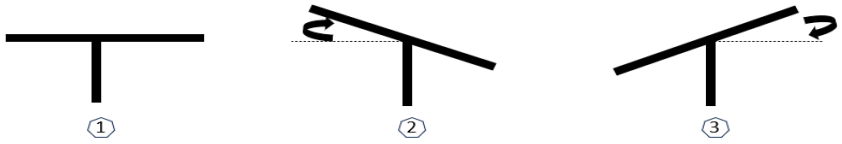

Figure 8: Nonlinear system response visualisation

This Figure shows the motion of the solar panel after implementation of the step input. Case one is when the model is at equilibrium at zero degrees. When the sun moves with a step input, the solar adjusts to try and keep capturing maximum sun. While it is trying to adjust it overshoots and reach 1.8 degrees in 3 seconds this is shown by case. Then it tries to adjust again to control this overshoot ending up undershooting this is shown by case 3. It then keeps on oscillating in the damped manner until it reaches the equilibrium point which is around 1.2 degrees.

4.1.2 Frequency domain

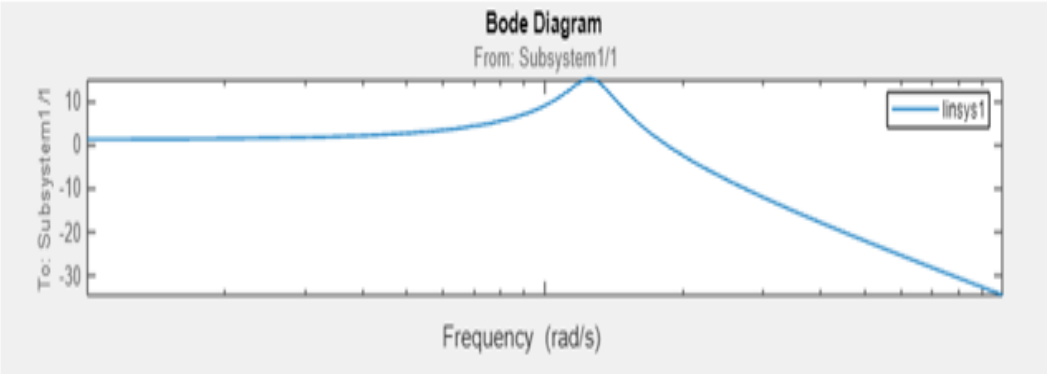

Figure 9: Non-linear response with frequency.

The Figure shows that the magnitude is always negative, and it becomes more negative as frequency increases. This means that the system is unstable and does not meet the frequency specifications.

4.2 Linear Plant

The non-linear model was linearized to find both time and frequency domain. This linear would allow for comparison of responses of linear and non-linear. The linearization allows for analysis of simple model but still representing the real model. From the correctly linearized model stability and behaviour of the real model can be predicted. This section presents the responses of the linearized model from a step input.

4.2.1 Time domain

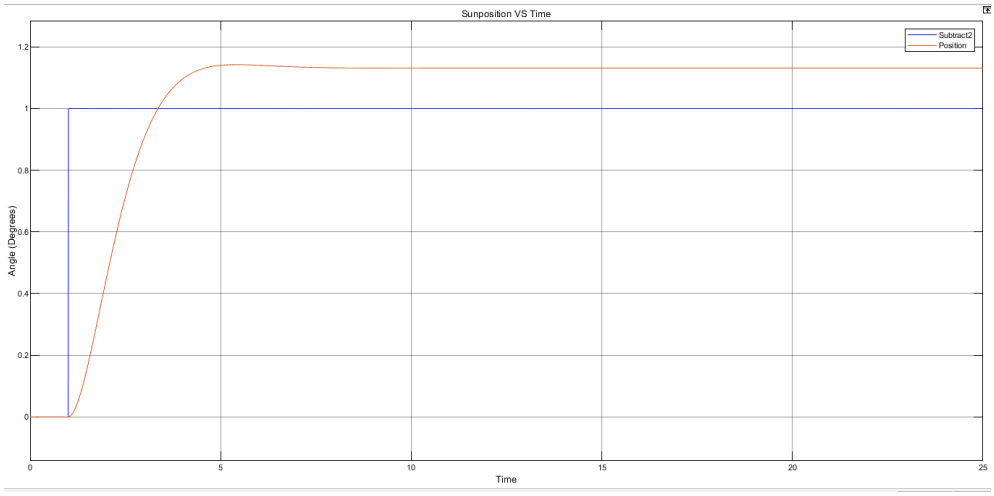

Figure 10: System response due to input

From the Figure it could be seen that that when there is an abrupt change in input the system stability is disturbed. The system response shoots up from zero degrees to 1.2 degrees for 5 seconds. After 5 seconds the system response becomes constant staying at that 1.2 degrees. The system after reaching equilibrium point it stays at equilibrium until there is another abrupt change in the input again.

- System response visualisation

Figure 11: Linear response visualisation

This Figure shows the motion of the solar panel after implementation of the step input. Case one is when the model is at equilibrium at zero degrees. When the sun moves with a step input, the solar adjusts to try and keep capturing maximum sun this is shown by case 2. After 5 seconds the model will reach equilibrium again and remain at 5 degrees.

4.2.2 Frequency domain

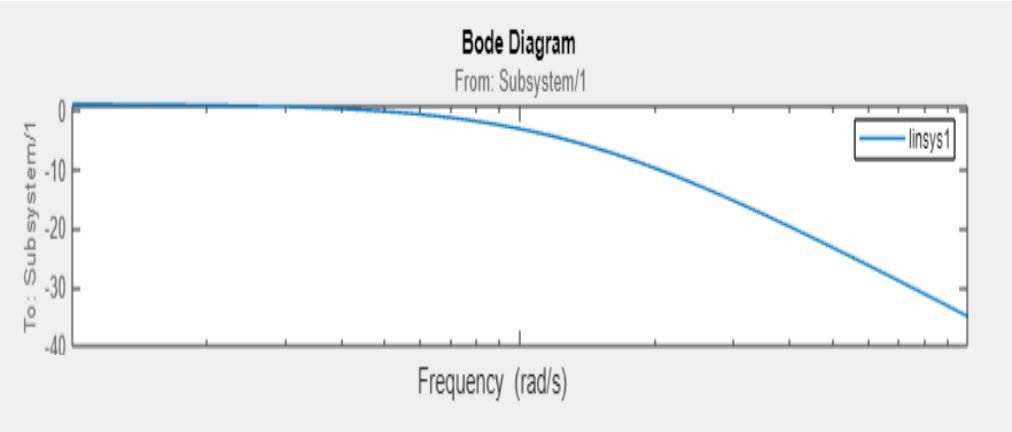

Figure 12: Linear response with frequency

The Figure shows that the magnitude is always negative, and it becomes more negative as frequency increases. This means that the system is unstable and does not meet the frequency specifications.

4.3 Linear vs Non-linear Plant

For time domain, when there is a step input, they both respond to it. The non-linear gave an oscillatory response in a damped manner and it was converging to 1.2 degrees while the linear overshoot and reach 1.2 degrees. There is a good correlation between both models hence the linearized equation has high accuracy. This is because small angle approximation was assumed hence good approximation. This means that the linearized model can be used as a replacement for real plant model for further analysis.

For both analysis of the models when the step input is inserted the system was responding in an undesirable. This showed that both systems are unstable. This also showed that both systems are not matching the expected performance specifications. This implies that the controller should be implemented as it is important to maintain the stability of the system and achieve the expected performance specifications. Adding a feedback loop to the system plant can help in eliminating the need for control. By using feedback loop the system shows stability but it converges after some time which is not very efficient. Another alternative to eliminate control is changing the system parameters but this might result in unrealistic model. Therefore, the controller is needed for stability and performance.

Performance of sun following without PID:

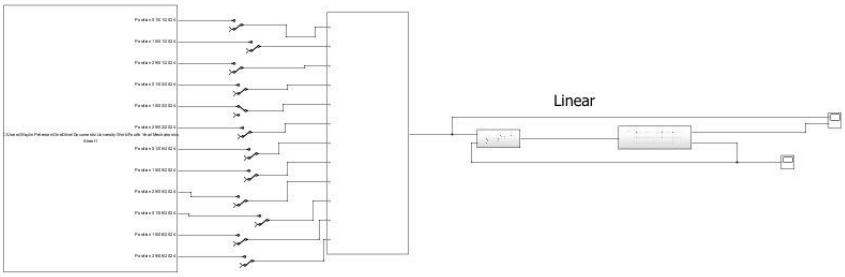

Figure 13: Block Diagram with sun data as input

5. Systems stability analysis

5.1 Stability Analysis of the linearized model

Stability analysis was performed for linear model using transfer of the system. The stability analysis allows for evaluation of how the system responds to the inputs signals and help in concluding if whether the control is necessary or not. The analysis was performed using different criteria and the results are resented in this section.

5.1.1 Pole-zero plots stability criterion

This criterion represents zeros and poles of the transfer function of the system graphically in the complex plane, making it easier to evaluate stability analysis. The zeros are values in s-plane where transfer function becomes zero. These values represent frequences of the system that gives zero response to input signals. The poles are values where transfer function becomes infinite. These values represent frequences of the system that gives infinite response to input signals.

- **Zeros**

Because the transfer function has numerator that is constant it means it has zeros at s=0.

- **Poles**

Taking the roots of the open loop transfer function gives the following results:

s_1 = -0.1696 + 1.9186i

s_2 = -0.1696 – 1.9186i

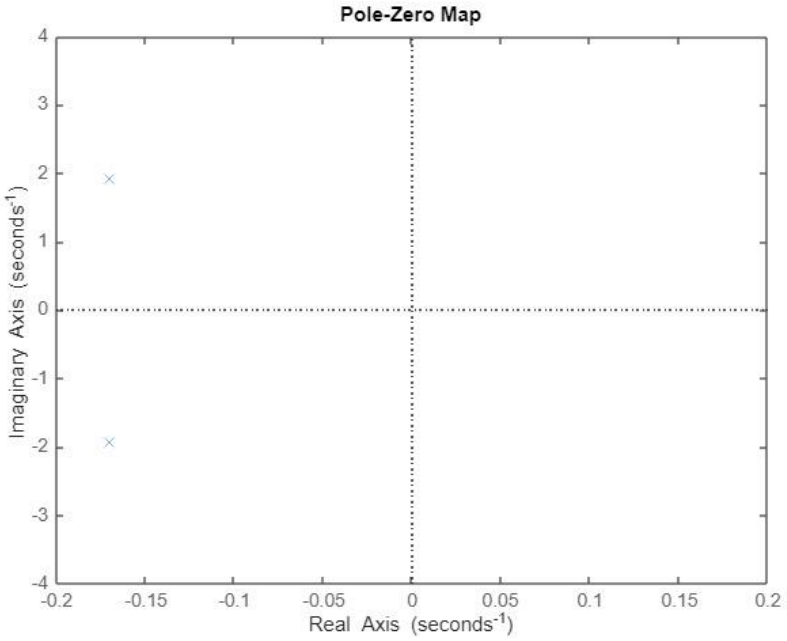

Figure 14: Pole-Zero Map

- **Discussion**
    1. The transfer function has zeros that lie on the origin of the plane, it also has 2 poles that have2 complex roots where one lies on the second quadrant and the other one lies on the third quadrant.
    2. Because the real parts for all poles are negative, all poles lie on the left half-plane, the stability of the system is guaranteed.
    3. The stability of the system means that if there is a disturbance to the system, the system will naturally converge towards its equilibrium over time without control inputs.

5.1.2 Routh-Hurwitz stability criterion

This is another criterion that was used to investigate the stability of the model. The drawback of this criterion is that it requires a closed-loop system characteristic equation to determine the stability. The advantage is that it allows the analysis of stability without the need to solve the roots of the characteristic equation.

The overall combined nonlinear equation of the system is:

$$G(s) = \frac{\theta(s)}{V(s)} = \frac{\frac{G_r k_t}{L_s + R}}{[(J_p)s^2 + (C_p + G_r^2 C_m)s + (\frac{k_e G_r^2}{L_s + R} - yF_g)]}$$

The above transfer function derived to give the following characteristic expression to be analysed:

$$(J_p)s^2 + (C_p + G_r^2 C_m)s + (\frac{k_e G_r^2}{L_s + R} - yF_g)$$

To perform the analysis, The Routh array is constructed by arranging coefficients of the expression in a tabular format.

Table 4 Routh Table

s^2	J_p	$\frac{k_e G_r^2}{L_s + R} - yF_g$
s^1	$C_p + G_r^2 C_m$	0
s^0	$\frac{k_e G_r^2}{L_s + R} - yF_g$	0

- **Discussion**
    1. Examining the first column terms, when all the constants are substituted, the values have shown to always come back being positive.
    2. This means that all the roots of the characteristic expression lie on the left half-plane, ultimately meaning that the model of the system is stable.
    3. This analysis correlates with the analysis of zero-pole plots which was made in section 5.1.1.
    4. Because the open loop system is stable, the close loop system is also stable.

5.1.3 Nyquist criterion

Another criterion that was used to investigate the stability of the system is Nyquist criterion. This criterion allows the evaluation of stability of the model using the open loop transfer function. The Nyquist that was obtained based on the defined transfer function in section 5.1.2 is shown in Figure 20.

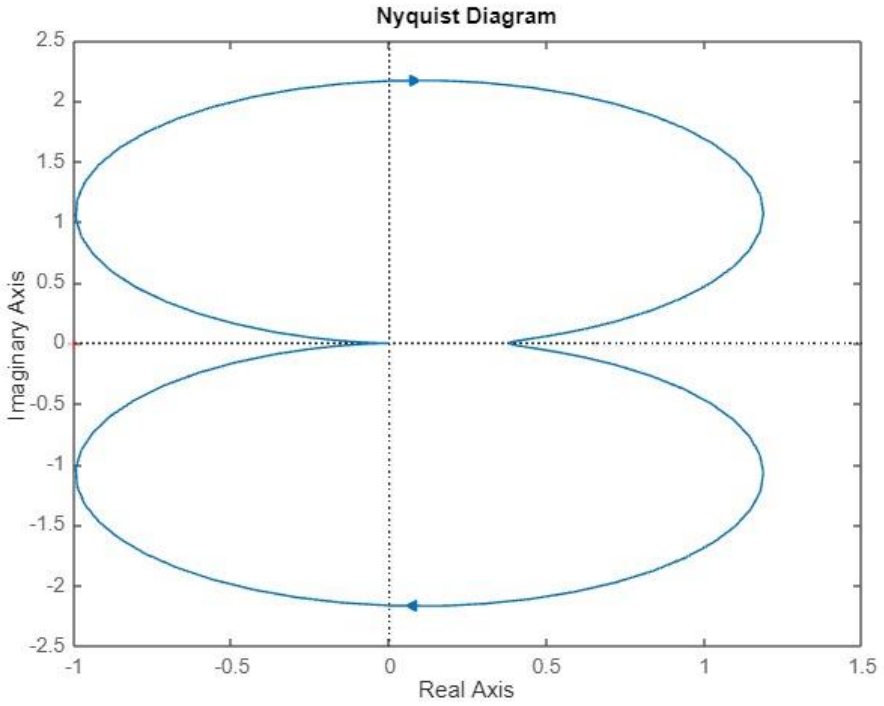

Figure 15: Nyquist diagram

- **Discussion**

1. The Nyquist plot does not come close to the point (-1, 0i), therefore the model is stable.
2. Because the plot is not too close to the point (-1, 0i), there is adequate relative stability on the model.
3. The results of this criterion also correlate with previous criteria.

5.1.4 Bode Plots stability criterion.

Another criterion that was used for investigation is bode plots. This criterion provides the graphical presentation of system response in frequency domain allowing for analysis of stability margins. The results obtained from analysis are shown in Figure 21.

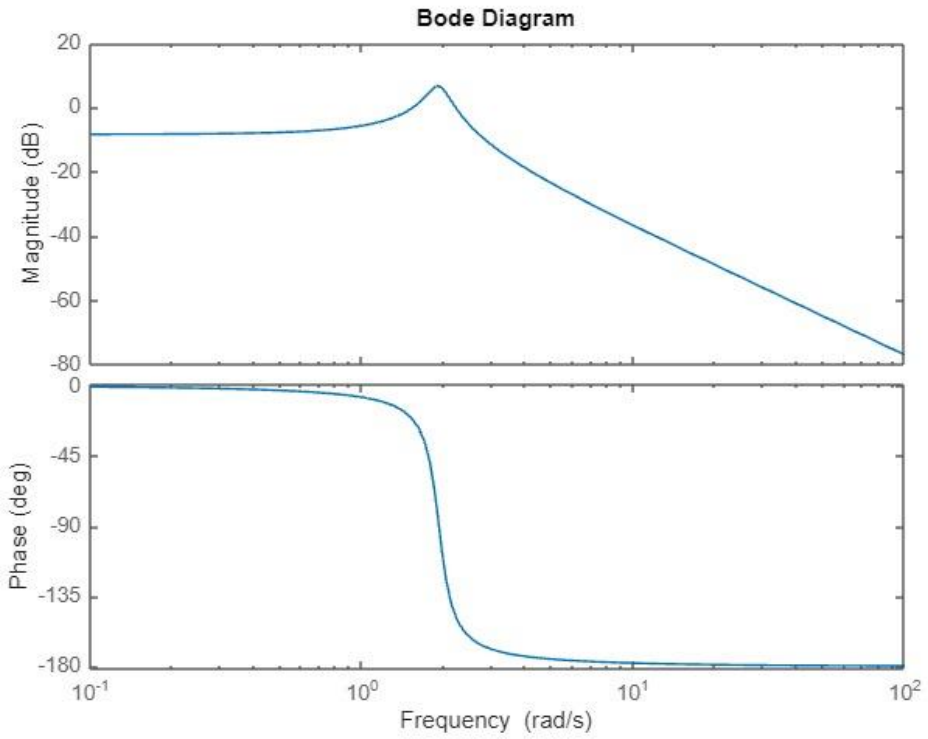

Figure 16: Bode diagram

- **Discussion**

1. It is evident from Figure 25 that for all frequences the magnitude is negative implying instability.
2. The phase is also negative implying instability.
3. Therefore, the system according to this criterion is unstable.

5.1.5 Conclusion

According to poles-zero, Routh-Hurwitz and Nyquist the system is stable but according to bode plots it is unstable. To correct for instability the control will be necessary.

5.2 Stability Analysis of the non-linearized model

Unlike linear model which can be analysed using analytical criteria, analysing stability of non-linear model using analytical criteria is difficult due to complex and nature of the system being dynamic. Therefore, the analysis of stability for this model was performed using numerical method Simulink. The time responses from the Simulink presented in section 4.1 were used for evaluation of stability. Based on the results obtained in the Simulink the system is unstable and correlates with the conclusion made from linear model.

The need for a control system in this design is based on several reasons. The main objective of this design is to design a model that can follow the sun and maximize the photoelectric effect by converting solar energy into stored/potential energy. The need for a control system stems from the main objective to effective track the sun. To maximize the stored energy the panel needs to be perpendicular relative to the sun, however, this is not seen based on the model. The system however is always 5% of the target position (the penal needs to be perpendicular to the sun). This is just one validation as to why a control system is required:

- Reduction of Non-linear Effects: Closed-loop systems reduce non-linear effects commonly seen in open-loop systems, improving overall performance.
- Noise and Disturbance Reduction: These systems minimize external noise and disturbances, enhancing accuracy.
- Increased Efficiency and Quality: By continuously monitoring and adjusting the output, closed-loop systems boost efficiency, accuracy, and quality.
- Stability: Closed-loop systems stabilize dynamics and reduce process uncertainties.

When sunlight intensity increases, sensors relay data to a PLC (Programmable Logic Controller), which adjusts the panel's position via a motor to maintain alignment with the Sun. Accurate alignment ensures maximum energy capture and efficiency.

A control system is crucial for a solar tracking system to maintain an error of less than 1%. It ensures precise adjustments based on sunlight intensity and position, leading to optimal energy production. Without a control system, the alignment would be inaccurate, reducing efficiency and energy output.

Both closed-loop control systems and control systems in solar tracking are vital for enhancing performance, reducing errors, and improving stability and efficiency.

6 Design of controller

Based on the stability analysis undertaken for the system, it was found that it was necessary for the controller to be implemented. Implementation of the controller will ensure that the system will be able to stabilize and conforms with the required specifications. The angle of the panel to allow maximum harnessing of the sun is of interest as this is the main objective of the project and thus the controller should ensure that the desired suitable angle is achieved at all times based on the suns positioning.

6.1 Implementation of Proportional Integral Derivative control (PID)

Proportional Integral Derivative control incorporates the use of proportional, integral, and derivative gains. The controller with the combination of the gains has more advantage and capabilities as each individual gain advantage is added to the system [9]. The controller with combination of the gains is given by the following equation:

$$u(t) = K_p e(t) + \frac{K_p}{T_i}\int_0^t e(t)\,d(t) + K_p T_d \frac{de(t)}{dt} \tag{6.1}$$

K_p: Proportional Gain

T_i: Integral Time

T_d: Derivative Time

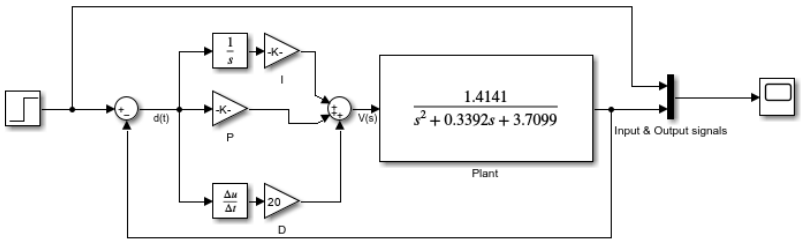

Figure 17: PID controller Block diagram.

The desired input angle was used for PID analysis, the system response to the input is also of interest as this shows clearly how the system will react to the certain imposed input. The angle input of 28.65° was used in the implemented controller with the aid of proportional integral and derivative controller, the system which was producing a large steady state error and initially unstable was able to stabilise after a certain period of time. The system was stabilised with the use of proportional, integral, and derivative gain blocks.

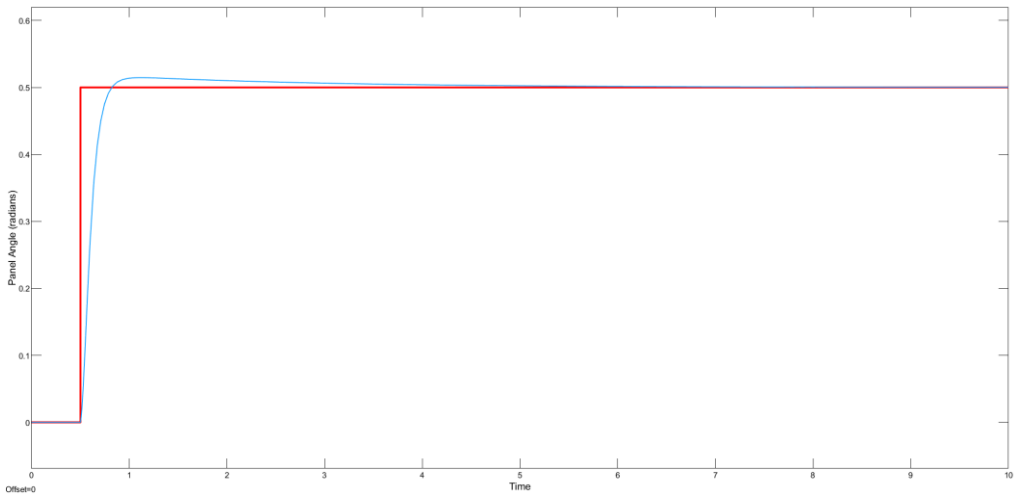

Figure 18: System response to input and PID.

Table 3 below highlights the specifications of both the PID controlled, uncontrolled and the desired specifications that will allow the system to perform ideally. The uncontrolled system specifications deviate more from the desired specifications of the system. The implementation of the controller was to lower the deviations from the uncontrolled system such that they will fall within the range of the desired specifications. The addition of the PID controller to the system and set gains greatly reduced the specifications from the uncontrolled system to fall within the range of the desired specifications for the system to perform ideally.

Table 5: Desired specifications as compared to PID gain specifications.

Specification	**PID controlled**	**Uncontrolled**	**Desired**
Maximum Overshoot	8.21 %	75.7 %	$\leq 15\%$
Peak	0.11 rad	0.67 rad	$< 0.5rad$
Settling time	0.298s	23s	$< 2s$
Rise time	0.0396s	0.58s	$< 0.5s$
Steady state error	1%	0.381%	5%

The system performance or response is greatly affected by the input voltage to the motor, this then needs to be correctly controlled and monitored as to ensure ideal response of the system from the motor input voltage. The limits of [-12,12] were set for the saturation n of the motor as to control the voltage input to the system for optimal operation and response.

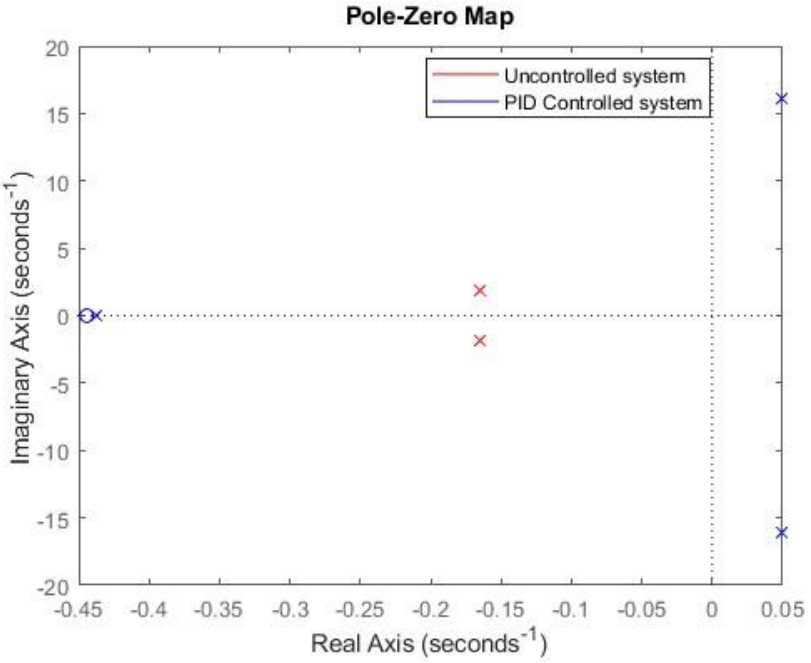

Figure 19: Pole-zero map for both uncontrolled and PID controlled systems.

Figure 3 above shows the pole-zero map which includes both uncontrolled and PID controlled systems, the map shows the stability of both the systems. The map shows the poles of the PID controlled system to be on the right of the s-plane, this highlights that the system is still unstable even after the use of the PID and more tuning on the system is thus required.

6.2 Root Locus Method

The root locus method will be used to improve the PID or PDF by providing a graphical representation of the closed-loop system's pole locations as the gain of a feedback controller varies. This analysis helps us understand the stability and performance of the control system, allowing us to adjust and optimize the controller for better overall performance. The root locus method also aids in visualisation of the systems stability based on its ability to graphically represent a closed loop system in a pole zero map.

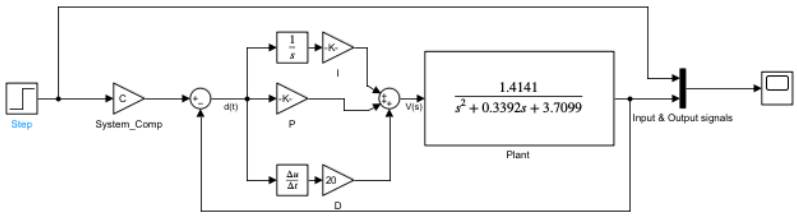

Figure 20: PID controlled system with root locus gain added.

The transfer function of the plant which has PID controller returned the following equation:

$$\frac{\theta_p(s)}{V_s(s)} = \frac{127.3 + 56.56}{s^3 + 0.3392s^2 + 258.2s + 113.1}$$

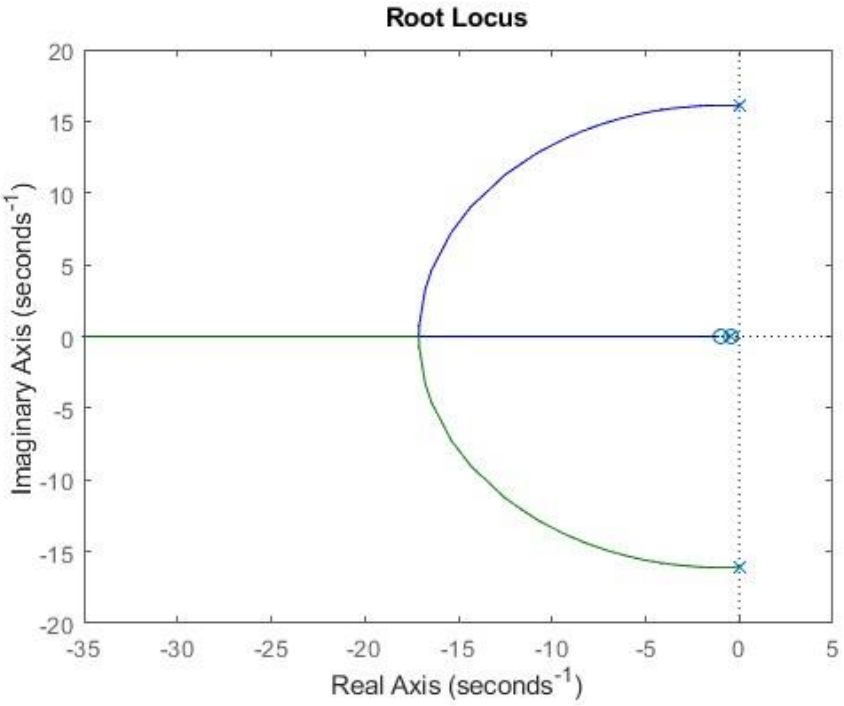

Figure 21: PID Controlled root locus plot.

The root locus plot in Figure 9 shows that the system is marginally stable with the poles lying on the imaginary axis and this makes the system neither stable nor unstable.

7 Critical evaluations of the system and simulation

The designed system should be evaluated to assess its functionality and if it meets all system required specifications. The implemented controllers and method used in analysing the system should also be evaluated to assess their effects and reliability of the designed system. The derived mechanical equations which resemble the functionality of the system mechanical were supposed to be incorporated into the system together with motor as the electrical part of the system. All the controllers are imperative for optimal functionality of the system as the controllers ensures that the system can be able to do account for disturbances and thus enhance performance.

7.1 Stability analysis

Stability analysis was performed to ensure if the system will be able to stabilise without the control. The analysis is imperative as there was not going to be a need for the controller if the system was able to stabilise. Implementation of the controller was going to be void if the system was able to stabilise on its own, there was going to be resource loss and costs incurred unnecessarily. The stability analysis did highlight that the system on its own will not be able to stabilise and perform optimally according to the required specifications thus a controller was needed to ensure optimal performance of the system. For the stability analysis, several criteria were used to determine which one conforms with the ideal stability and instability of the system.

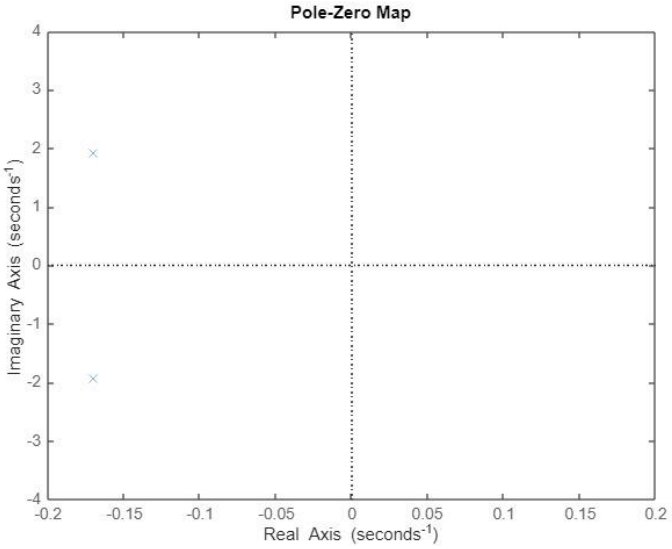

Figure 22: Pole-zero Map

The pole zero plot in figure 22 shows that the system is stable as the poles are on the left side of the s plane, the Routh Hurwitz also showed that the system is stable and this correlates with the zero-plot map that the system is indeed stable. The Nyquist was also used for evaluation and the plots obtained conforms with the system being stable. The bode plots also showed all frequencies magnitude and phases is negative and it indicates that the system is stable. From the four evaluated criteria, one showed that the system is unstable and can therefore the system was found to be unstable. Implementation of the controller is necessary to correctly stabilise the system.

7.2 Stability and control

The designed model should enable the solar to track the sun for maximum harnessing of the sunlight. Sun positioning at different hours of the day should be used for proper control and positioning of the panel. Model control should then be implemented with suns positioning at different times of the day in mind as this will keep the solar panel at the right position for each certain period. It was imperative that the sun data be obtained to correctly visualize the suns positioning and allowing correct adjustments of the panel in conjunction with the sun positioning. The suns data was used as input to the system and the systems response to the input which was used as the suns data was also evaluated.

The controller was then needed to correctly stabilise the systems response to the input, which is the suns data and correctly position the panel in response to the suns positioning at all times.

The Proportional Integral Derivative (PID) controller was implemented for stages of the system that needed stabilisation. The use of PI was initially explored to test its validity in stabilising the system and reduction of the steady state error. The PID was used for ideal stabilisation and overall system and reduction of the systems stability. The PID was further tuned with the use of root locus for enhanced performance and further reduction of the steady state error to allow the system to perform ideally and conform.

9 Conclusion

The objective of the assignment was to design a solar panel system for Apex student's accommodation in Braamfontein. This system was design with primary goal of capturing maximum sunlight at every time. After the system was designed, it was analysed to correctly stabilise and ensure optimal performance of the system and correct tracking of the sun for maximum harnessing of the sunlight. The stability analysis of uncontrolled model proved that the system is unstable. The analysis response without a controller was not correlating with expected performance specifications. To maintain stability and match expected specifications the controller was implemented. The controllers that were used are PID and root locus. The use of PID was to reduce the steady state error to ensure ideal operation of the system and reduction of the steady state error. Tuning of the PID was further done with the aid of root locus and the steady state of the system was further reduce significantly. The PID and root locus were also used for the system without the sun tracking data to tests and validate the behaviour of the PID which was then further implemented in the system with the sun data for correct and efficient tracking of the sun.

The linear model proved that it can be used as a replacement for non-linear model which represents the real system with high confidence of accuracy. This then gave insight that the linearity of the system will yield appreciable results of the model and mimic the real-life application.

Omission and assumptions made through the process of model analysis can thus however significantly affect the results as other factors might have been clouded this having significant impact in the overall system which can lead to inefficient operation of the controller and the system.

References

[1] D. A. Panday, “MECHATRONICS II: MECN4029A - PROJECT ASSIGNMENT,” University of Witwatersrand, Johannesburg, 2024.

[2] NEXG POWER, “NEXG POWER,” [Online]. Available: https://nextgpower.com/how-exactly-does-a-battery-storage-system-with-a-hybrid-inverter-work/. [Accessed 05 May 2024].

[3] H. P. C. S. Ozcelik, “Two-Axis Solar Tracker Analysis and Control for Maximum Power Generation,” *Procedia Computer Science*, vol. 6, pp. 457-462, 2011.

[4] H.-U. Oh, “CubeSat’s Deployable Solar Panel with Viscoelastic Multilayered Stiffener for Launch Vibration Attenuation,” International Journal of Aerospace Engineering, Korea, 2022.

[5] ENF, “ Solar Panel Directory,” ENFSOLAR, 2024. [Online]. Available: https://www.enfsolar.com/pv/panel-datasheet/crystalline/49147?utm_source=ENF&utm_medium=panel_list&utm_campaign=enquiry_product_directory&utm_content=9427. [Accessed 10 05 2024].

[6] E. Glueck, “Bodine Electric Company,” 02 November 2021. [Online]. Available: https://www.bodine-electric.com/blog/bodine-gearmotor-constants/. [Accessed 08 May 2024].

[7] D. A. Panday, “MECN 4029A MECHATRONICS II Class Notes Chapter 1 – Chapter 2,” School of Mechanical, Industrial and Aeronautical Engineering, Johannesburg, 2024.

[8] C. W. Silva, “9.3 Control of DC Motors,” in *Mechatronics An Integrated Approach*, Washington, D.C., Taylor & Francis Group, 2011, p. 788.

[9] K. Ogata, Modern Control Engineering, New Jersey: Prentice Hall, 1997.